**Zeitschrift:** Schweizerische mineralogische und petrographische Mitteilungen = Bulletin suisse de minéralogie et pétrographie

**Band:** 83 (2003)

**Heft:** 2

**Artikel:** Tectono-metamorphic evolution of the Frontal Penninic units of the Western Alps : correlation between low-grade metamorphism and tectonic phases

**Autor:** Ceriani, Stefano / Fügenschuh, Bernhard / Potel, Sebastien

**DOI:** https://doi.org/10.5169/seals-63139

*Schweizerische Mineralogische und Petrographische Mitteilungen 83, 111–131, 2003*

# Tectono-metamorphic evolution of the Frontal Penninic units of the Western Alps: correlation between low-grade metamorphism and tectonic phases

*Stefano Ceriani*[1], *Bernhard Fügenschuh*[1], *Sebastien Potel*[2] and *Stefan M. Schmid*[1]

**Abstract**

The frontal Penninic units (FPU) of the Western Alps underwent a complex tectono-metamorphic evolution during Alpine orogeny that can be divided into three major stages: a first one pre- to syn-collisional (D1 and D2), a second one (D3) and third one (D4) post collisional. This study aims to integrate detailed structural mapping with metamorphism (Kübler index and K-white mica *b*-cell dimension analysis) and thermochronology (fission track analysis).
Metamorphic conditions in the FPU range from high anchizonal to epizonal conditions. The highest metamorphic temperatures (~300 °C) were deduced for the Houiller unit and the Cheval Noir unit. Structural analysis and fission track ages indicate that the temperature peak in the Houiller unit was reached during D1, i.e. in the Eocene. The metamorphic peak in the Cheval Noir unit was reached during D2 due to overthrusting of the more internal Subbriançonnais and Houiller units.
Kübler indices and fission track data show a vertical gradient within the Cheval Noir unit with the higher temperatures recorded at the base of the stratigraphic series. This metamorphic gradient was successively folded during D3 in the Oligocene.
The K-white mica *b*-cell dimension values do not show major differences within the FPU units. They present a clear bimodal distribution interpreted to be due to the superposition of the effects of the two stages of deformation. The K-white mica *b*-cell dimension values from the FPU are higher than those recorded in the Dauphinois domain indicating that the FPU were subjected to higher pressures compared to the Dauphinois domain. Metamorphism in the Dauphinois domain, which is affected by one major phase of deformation (i.e. D3) only, is related to the overthrusting of the FPU along the syn-D3 Roselend thrust.
According to our tectonic reconstruction the first two phases of deformation (D1 and D2) developed during subduction of the Valaisan units, within the accretionary wedge. Our data indicate that metamorphism affecting the FPU south of Moûtiers is mainly related to the first stage (D1 and D2) when the FPU formed the frontal and upper part of the Alpine accretionary wedge.
The second stage (D3), characterized by thrusting and folding, developed during the Oligocene in a post-collisional scenario and led first to low T–low P metamorphic overprint and finally to a partial exhumation of the FPU already in the Late Oligocene.

*Keywords:* Kübler index, K-white mica, *b*-cell, fission track dating, tectono-metamorphic evolution, Western Alps.

## 1. Introduction

The Frontal Penninic Units south of Moûtiers (FPU) comprise, from internal towards external, the Houiller unit (zone Houllière, part of the Briançonnais paleogeographic domain), the Subbriançonnais unit and the Cheval Noir unit (Fig. 1). The latter was formerly attributed to the "Ultradauphinois", but is now interpreted to represent an accretionary wedge deposited above the Valais (or North-Penninic) suture zone (Ceriani et al. 2001). All three tectonic units mainly consist of detrital and/or carbonatic sediments. North of Moûtiers, the Valaisan units occupy a tectonic position similar to the Cheval Noir flysch unit (see Fig. 1 and discussion in Ceriani et al., 2001). The low-grade metamorphic FPU are situated between the highly deformed and higher-grade metamorphic internal Penninic units in the east (e.g. Internal massifs and South-Penninic schistes lustrés), and the less deformed Dauphinois paleogeographic domain in the west representing the European passive margin bordering the Valais ocean. Hence, the FPU represent the most exter-

[1] Departement Erdwissenschaften, Universität Basel, Bernoullistr. 32, CH-4056 Basel, Schweiz. <Stefano.Ceriani@unibas.ch>, <bernhard.fuegenschuh@unibas.ch>, <Stefan.Schmid@unibas.ch>
[2] Institut für Geowissenschaften und Lithosphärenforschung, Senckenbergstr. 3, D-35390 Giessen. <Sebastien.Potel@geolo.uni-giessen.de>

0036-7699/03/0083/111 

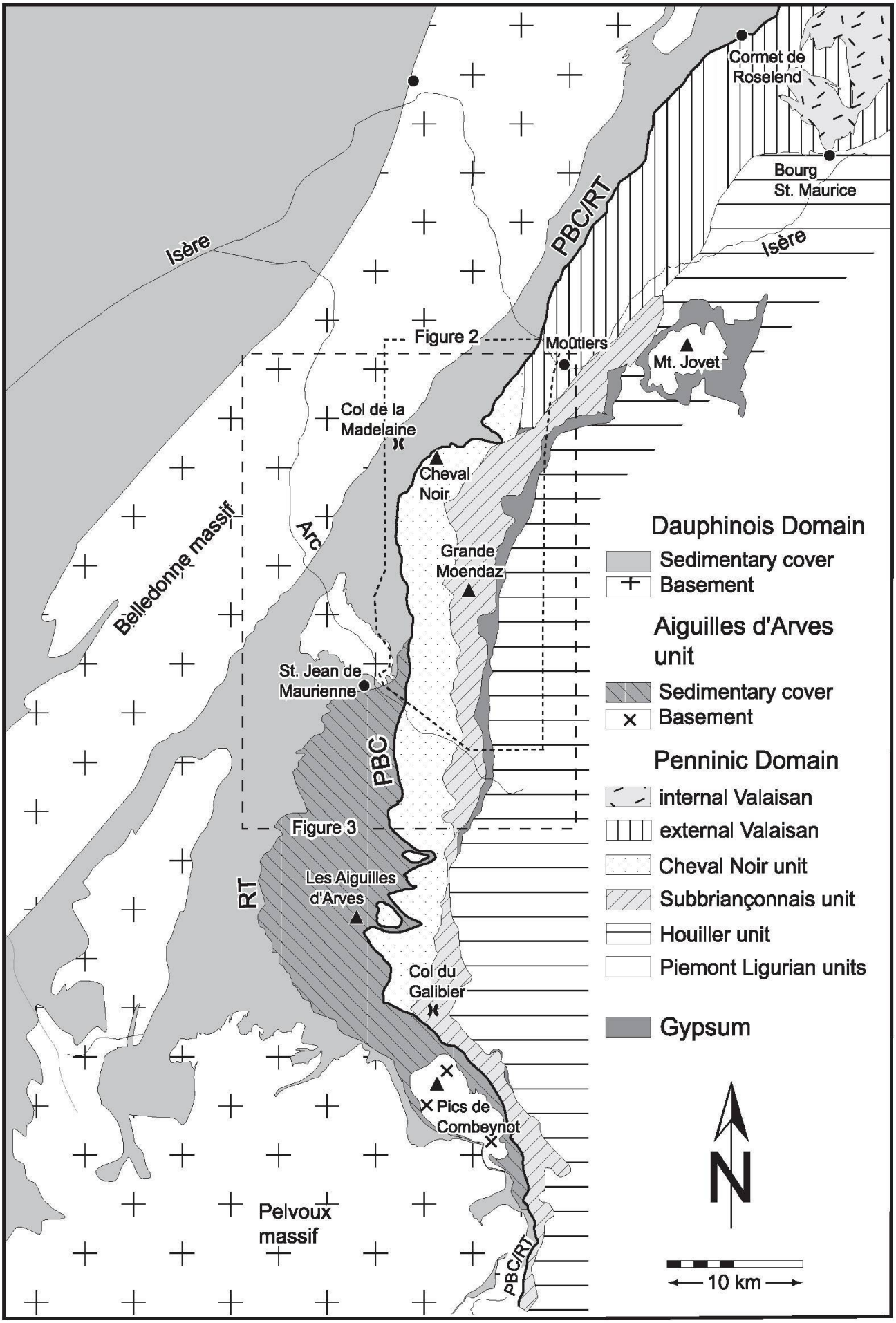


*Fig. 1* Tectonic map of the area between the Cormet de Roselend and the Pelvoux Massif (Western Alps). Boxes indicate the areas covered by Figures 2 and 3. PBC — Penninic Basal Contact; RT — Roselend Thrust.

nal parts of the Alpine accretionary wedge. However, they underwent a complex polyphased tectono-metamorphic evolution during Alpine orogeny.

In view of their frontal location, the FPU represent a key area for studying differences and/or similarities in the tectonic evolution of the Penninic units with respect to the Dauphinois domain, i.e. the European margin. Moreover, the reconstruction of the tectono-metamorphic evolution of the FPU provides important constraints for understanding the evolution of the western Alps. However, the FPU units were poorly studied until very recently. Ceriani (2001) undertook a first comprehensive structural and metamorphic study in the FPU, while Ceriani et al. (2001) analyzed the complex polyphase deformation history within the framework of the evolution of the Western Alps. Only very few metamorphic data are available from these units so far (see compilation in Frey et al., 1999). By focusing on low-grade metamorphism this study primarily aims to fill this gap.

Rocks from low-grade metamorphic units such as the FPU are, in most cases, only partially recrystallized. Hence, detrital minerals coexist with very fine-grained and newly formed minerals. Dis-equilibrium-types, such as illite and smectite, are also very common (Essene and Peacor, 1995). The combined metamorphic and structural study presented here, carried out with the aim of reconstructing the tectono-metamorphic evolution of the FPU, used three different methods to determine metamorphic grade of the FPU between the Arc and Isère valleys. The measurement of illite crystallinity and fission track data helped to constrain the temperatures, while the measurement of the K-white mica *b*-cell dimension provided pressure estimates.

The first of these methods is an easy, fast and well-tested technique in determining the metamorphic grade in low-grade metamorphic terrains (Frey and Robinson, 1999). Crystallinity of clay minerals is primarily a function of temperature. The chemical reactions responsible for the degree of crystallinity in clay minerals are not equilibrium reactions. As a consequence, no absolute temperature values can be provided using this method (Frey and Robinson, 1999; Mullis et al., 2002). The second method, i.e. fission track analysis was successfully used to study the final part of the exhumation history of the FPU (Fügenschuh and Schmid, 2003). However, in units that only underwent low-grade metamorphic overprint the annealing behavior of fission tracks can be used, in combination with other techniques, for T-estimates. The third method, the measurement of the K-white mica *b*-cell dimension (Sassi, 1972; Sassi and Scolari, 1974) monitors variations in the *b*-cell dimension of K-white mica. This method is used as a comparative geobarometer in low-grade metapelitic rocks (Frey and Robinson, 1999).

In the present study, the application of these three methods was combined with detailed structural mapping of the area (see Ceriani, 2001, and Ceriani et al., 2001 for more details). This combined approach allows us to establish the timing of deformation and metamorphism within the Houiller, Subbriançonnais and Cheval Noir units, and to correlate these data with the neighboring Dauphinois domain.

## 2. Geological setting

The study area is situated between the Arc and Isère valleys, immediately south of Moûtiers (Western Alps, Savoie, France; see Fig. 1). The Frontal Penninic Units south of Moûtiers are, from west to east, the Cheval Noir, Subbriançonnais, and Houiller units (Fig. 1). Classically, the Cheval Noir unit has been considered as part of the Dauphinois domain. This unit consists of a thick series of Tertiary (mainly Priabonian) sediments (wildflysch, breccias and flysch) which rest on a Briançonnais type substratum (Serre et al., 1985; Ceriani et al., 2001). This substratum consists mainly of Permian conglomerates (Verrucano facies) and pelites overlain by Jurassic and Cretaceous sediments. We interpret the Cheval Noir unit to represent the remnants of a trench developed during the final stages of subduction, when the European plate reached the subduction zone (Ceriani et al., 2001). The Subbriançonnais unit is made up of marine Mesozoic sediments. It represents a continuous stratigraphic sequence starting with Upper Triassic dolomites and pelites and ending with Oxfordian shales. The Houiller unit largely consists of continental detrital sediments, i.e. Carboniferous coarse-grained sandstones and breccias interbedded with pelitic layers. Permian conglomerates and pelites, as well as Lower Triassic dolomites and pelites, are also present in this unit within the area studied.

In the west the FPU are separated from the Dauphinois domain by the Penninic basal contact (i.e. PBC in Fig. 1). The Dauphinois domain comprises basement (external crystalline massifs) and cover series. To the east of the study area the Houiller unit is in contact with a basement unit (i.e. Gneiss du Sapey) of the more internal Briançonnais domain. North of Moûtiers the Cheval Noir and Subbriançonnais units wedge out in map view (Fig. 1) and are "replaced" by the Valaisan

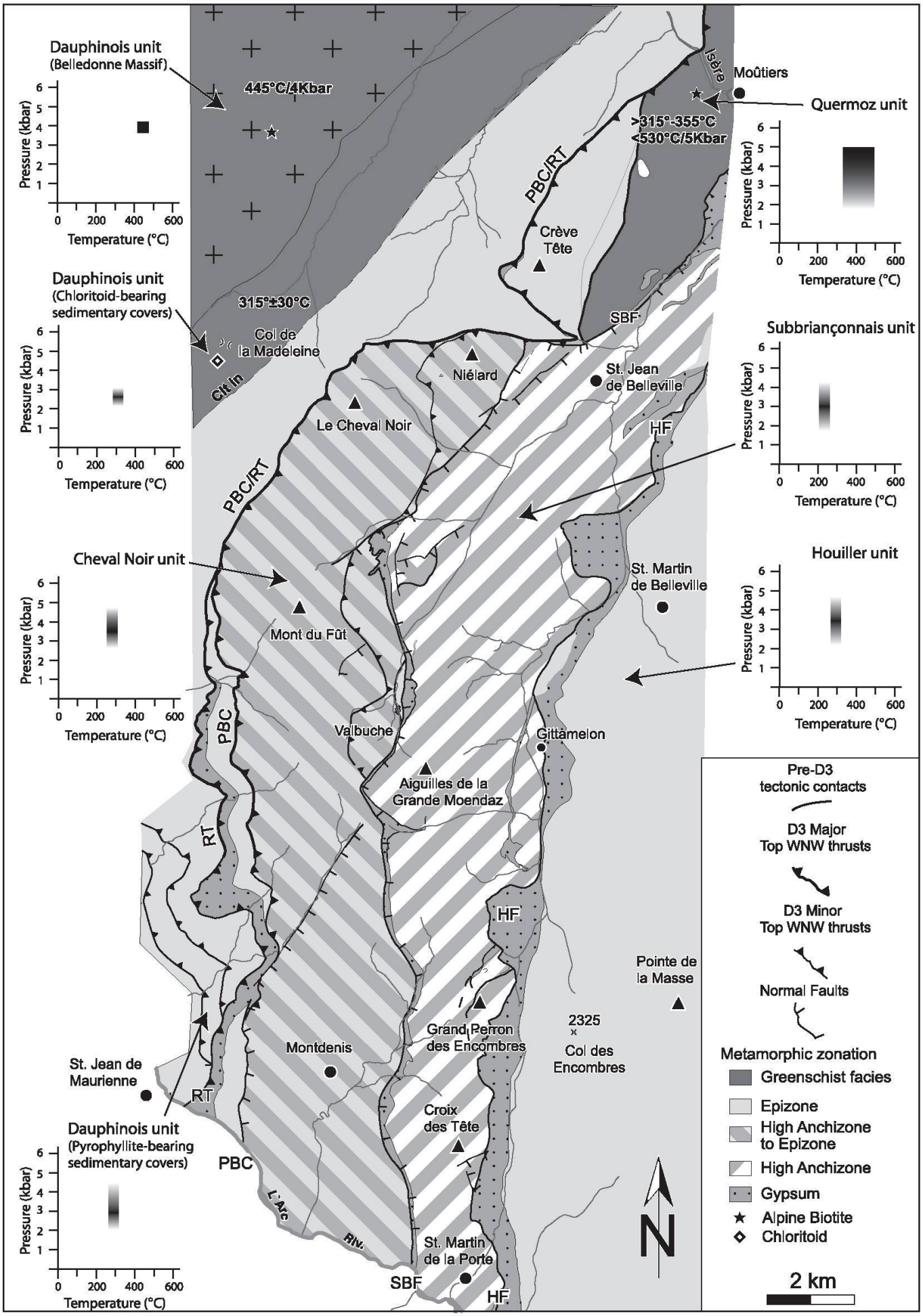
Dauphinois unit
(Belledonne Massif)
445°C/4Kbar
Dauphinois unit
(Chloritoid-bearing
sedimentary covers)
315°±30°C
Col de
la Madeleine
Cit in
Cheval Noir unit
Dauphinois unit
(Pyrophyllite-bearing
sedimentary covers)
Pressure (kbar)
Temperature (°C)
Isère
Moûtiers
Quermoz unit
>315°-355°C
<530°C/5Kbar
PBC/RT
Crève
Tête
SBF
Niélard
St. Jean
de Belleville
Subbriançonnais unit
HF
Le Cheval Noir
PBC/RT
Houiller unit
St. Martin
de Belleville
Mont du Fût
PBC
Valbuche
Gittamelon
Aiguilles de la
Grande Moendaz
RT
HF
Pointe de
la Masse
2325
Col des
Encombres
Grand Perron
des Encombres
Montdenis
St. Jean de
Maurienne
RT
Croix
des Tête
PBC
L'Arc
Riv.
St. Martin
de la Porte
SBF
HF
N
Pre-D3
tectonic contacts
D3 Major
Top WNW thrusts
D3 Minor
Top WNW thrusts
Normal Faults
Metamorphic zonation
Greenschist facies
Epizone
High Anchizone
to Epizone
High Anchizone
Gypsum
Alpine Biotite
Chloritoid
2 km

*Fig. 2*

units. To the south the Cheval Noir unit can only be followed up to the Col du Galibier area (Fig. 1), while the other two FPU can be traced all around the arc of the Western Alps.

### *2.1. Review of existing data on metamorphism*

Each of the Frontal Penninic units in Savoie (i.e. the Valaisan, Cheval Noir, Subbriançonnais and Houiller units, Fig. 1) underwent a distinct metamorphic evolution in spite of close similarities with respect to their tectonic evolution (Fügenschuh et al., 1999). The Valaisan unit is known to be characterized by a higher degree of metamorphism than the other FPU of Savoie (e.g. Goffé and Bousquet, 1997). The Valaisan units can be divided into internal Valaisan (i.e. Versoyen unit) and external Valaisan (i.e. Pt. St. Bernard, Roc de l'Enfer, Moûtiers, Quermoz, and Bagnaz units; see Fig. 1, Fügenschuh et al., 1999, and Loprieno, 2001). Both the Versoyen and the Pt. St. Bernard units underwent eclogite facies metamorphism (Schürch, 1987; Cannic et al., 1996; Goffé and Bousquet, 1997), while the rest of the Valaisan units only underwent greenschist facies metamorphism (Fig. 2, Gély and Bassias, 1990; Goffé and Bousquet, 1997; Fügenschuh et al., 1999).

Metamorphic conditions within the less strongly metamorphosed FPU south of Moûtiers (i.e. Cheval Noir, Subbriançonnais and Houiller units, see Fig. 1), however, are poorly known. Few data are available only from the Cheval Noir and Houiller units. Illite crystallinity studies carried out in the Cheval Noir unit indicate anchizonal metamorphic conditions near the Cheval Noir peak (Aprahamian, 1988) and south of the Arc valley (Deharveng et al., 1987). Epizonal to lower greenschist facies metamorphic conditions were established in the internal part of the Houiller unit (Desmons and Goffé, in Debelmas, 1989) while no data are available for the external part of the Houiller unit. No data at all exist from the Subbriançonnais unit.

Regarding the Dauphinois domain, a first metamorphic study in meta-sediments from the Col de la Madeleine area (Fig. 1) analyzed illite crystallinity (Aprahamian, 1988). This work reported a normal metamorphic gradient, which decreases from W to E, i.e. up-section. Anchizonal values are recorded in the west and at the base of the Dauphinois sediments (Col de la Madeleine area, see Fig. 1), while diagenetic values are observed further east, in the immediate footwall of the RT (i.e. the top of the Dauphinois domain). More recent studies have confirmed the presence of this E–W temperature gradient, but indicated higher metamorphic conditions (Gély and Bassias, 1990; Jullien and Goffé, 1993). Gély and Bassias (1990) estimated temperatures at around 445° C at 4 kbar (stilpnomelane + phengite = biotite + chlorite + quartz) for the Dauphinois basement in the Belledonne massif (Figs. 1 and 2). Moving east and into the Dauphinois sediments, biotite is absent while chloritoid is found within the Aalenian shales (Gély and Bassias, 1990; Jullien and Goffé, 1993). Vidal et al. (1999) estimated temperatures of 315 ± 30 °C for these chloritoid-bearing rocks of the Col de la Madeleine. Still further towards the top of the Dauphinois domain, i.e. from the Col de la Madeleine eastward (Fig. 2), chloritoid disappears while pyrophyllite appears within the Aalenian shales. In summary, all these indications show a decrease in temperatures within the Dauphinois domain from west to east, that is from base to top.

On a larger scale the Dauphinois domain also exhibits a north–south metamorphic gradient (Jullien and Goffé, 1993), with metamorphic conditions decreasing from the Cormet de Roselend area in the north to the Pelvoux massif in the south (Fig. 1). In the area between the Cormet de Roselend and the Col de la Madeleine (Fig. 1), the Aalenian shales of the Dauphinois domain are characterized by the presence of chloritoid. South of the Col de la Madeleine chloritoid is absent, while cookeite and pyrophyllite are found. Jullien and Goffé (1993) estimate temperatures of 280° to 340 °C and pressures lower than 4–5 kbar for the Dauphinois domain in the Col de la Madeleine area (Fig. 2).

In summary, the metamorphic grade decreases from west to east (i.e. from the base to the top of

*Fig. 2* Metamorphic map of the study area indicating the peak temperatures reached in the different tectonic units based on data given in Table 2 and on data from the literature (see text for details). Pressure-temperature diagrams indicate the metamorphic conditions inferred for the different units. Size of boxes indicates accuracy of the pressure and temperature estimation. The data for the Quermoz unit are from Gély (1989) and Gély and Bassias (1990). For the basement of the Dauphinois domain, P–T estimations from Gély and Bassias (1990) were taken, data for the sedimentary cover of the Dauphinois domain are from Leikine et al. (1983) and Vidal et al. (1999). Diagrams for the Houiller, Subbriançonnais and Cheval Noir units were derived from Kübler Index, fission track and b-cell dimension data of K-white mica of the present study. The boundary between greenschist facies and epizone in the Dauphinois was drawn along an isotherm marked by the appearance of chloritoid. HF — Houiller Front; SBF — Subbriançonnais Front; PBC — Penninic Basal Contact; RT — Roselend Thrust.

*Table 1* Correlation table indicating the age of the 4 main deformation phases. D1 and D2 are related to a first stage of sinistral transpression. D3 corresponds to a second stage of WNW-directed thrusting. D4 corresponds to recent normal faulting. Grey cells: no deformation observed.

| | | Dauphinois | RT | Cheval Noir | SBF | Subbriançonnais | HF | Houiller unit | Age |
|---|---|---|---|---|---|---|---|---|---|
| Third stage | $D_4$ | | | | normal faulting | | | | <5 Ma |
| Second stage | $D_3$ | Main cleavage & related folds ***Peak of metamorphism*** | Top WNW thrusting | Open folds with a poorly developed axial plane cleavage | Folded | Open folds with a poorly developed axial plane cleavage | Folded | Open folds with a poorly developed axial plane cleavage | Oligocene to Early Miocene |
| First stage | $D_2$ | | | Main cleavage Isoclinal folds ***Peak of metamorphism*** | Top N thrustung | Isoclinal folding with a strong axial plane cleavage ***Peak of metamorphism*** | Top NNW thrusting | Isoclinal folding with a strong axial plane cleavage | Priabonian (Eocene) |
| | $D_1$ | | | | ? | Main cleavage Isoclinal folds N-S stretching lineation | ? | Main cleavage Isoclinal folds ***Peak of metamorphism*** | pre-Priabonian >35 Ma (Eocene) |

the unit) in the entire Dauphinois domain east of the Belledonne massif. This gradient is superposed with a north–south gradient, with metamorphic grade decreasing from the Mont Blanc massif in the north to the Pelvoux massif in the south.

### *2.2. Tectonic history of the FPU*

The Frontal Penninic units south of Moûtiers underwent a polyphase tectonic history characterized by four deformation phases (i.e. D1, D2, D3 and D4). These four phases were divided into three major stages (Table 1) representative for the tectonic evolution of the whole Western Alps (Ceriani et al., 2001). A first stage comprises D1 and D2 and corresponds to deformation within an Alpine accretionary wedge. This stage, Eocene in age (Table 1), started before (D1) and lasted until the collision (D2) of the Briançonnais terrain (Briançonnais and Subbriançonnais together) with the European plate. Both D1 and D2 are characterized by north–south oriented stretching lineations, and both are responsible for the main penetrative deformation affecting the FPU. Isoclinal folds and a pervasive slaty cleavage developed in the rocks of the FPU during this stage. Structural field evidence indicates that all major thrusts between the different Frontal Penninic units (i.e. the thrusts labeled HF and SBF in Figs. 2, 3 and 4) were active during this first deformational stage.

The second main deformation stage affecting the FPU corresponds to D3 and is of Oligocene to Early Miocene age, see Table 1 and Ceriani et al. (2001). During this stage, the previously stacked FPU (comprising the Valaisan units), were thrusted on top of the Dauphinois domain along the RT (see Figs. 1, 2, 3, 4 and Ceriani et al., 2001). The structures related to this D3 deformation phase within the FPU are generally characterized by the development of a spaced crenulation cleavage. The main deformation in the Dauphinois occurred during this second stage, hence it correlates with D3 as defined in the FPU units (Ceriani et al., 2001).

Recent normal faulting (post-5 Ma, Fügenschuh et al., 1999) represents the third deformation stage. These normal faults (D4 in Table 1) are organized in two sets, trending NE–SW and N–S, respectively (Fügenschuh et al., 1999; Ceriani, 2001). In the area south of Moûtiers (Figs. 2 and 3), two major normal faults were mapped between the Subbriançonnais and the Cheval Noir units, a northern one trending NE–SW and a southern one trending N–S. Occasionally these normal faults reactivated former thrusts such as the SBF (Sue and Tricart, 1999) or the HF (Fügenschuh et al., 1999).

## 3. Illite Crystallinity and K-white mica *b*-cell dimension

Illite crystallinity (IC) was measured for 37 samples from the FPU (i.e. Houiller, Subbriançonnais

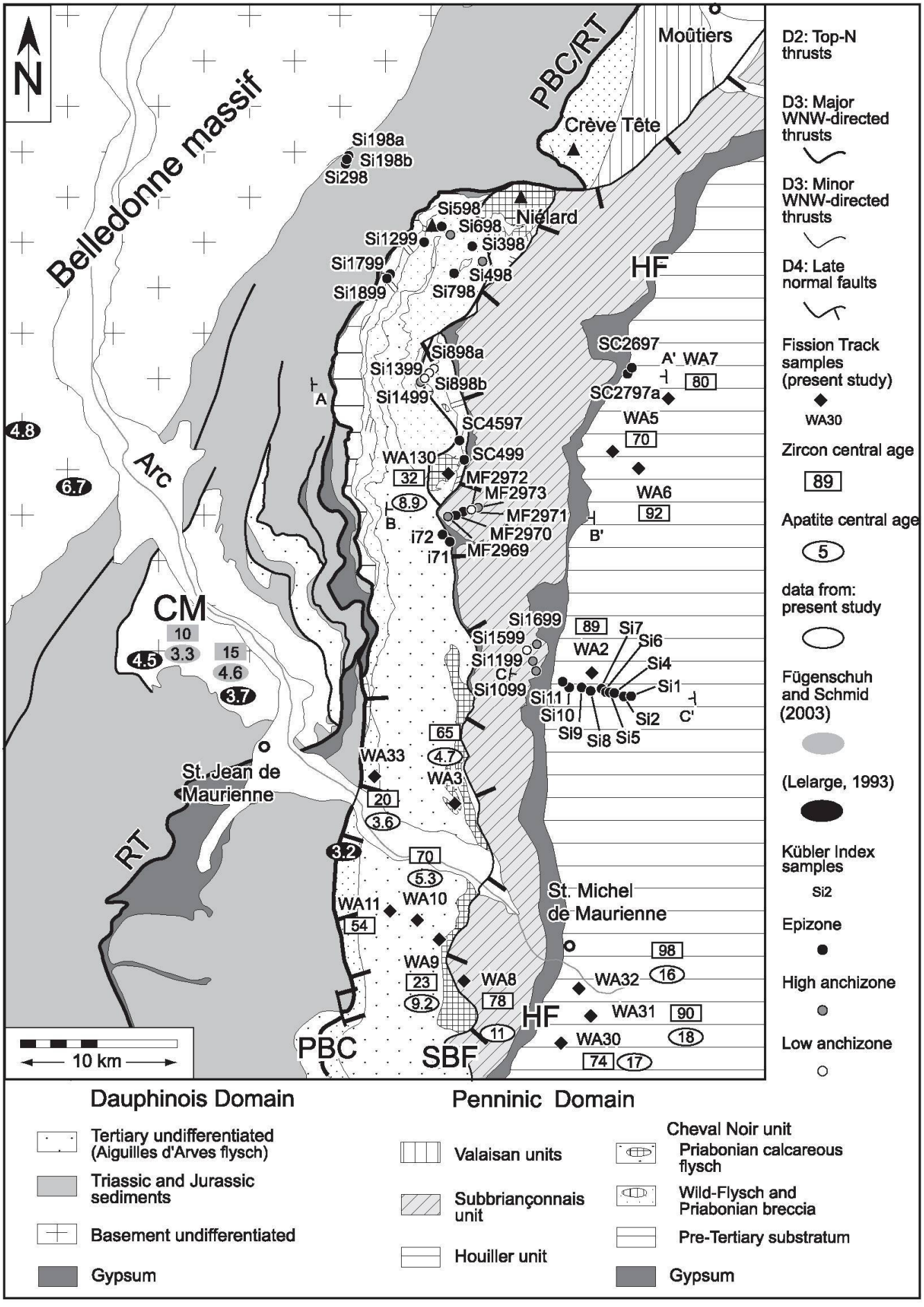


*Fig. 3* Tectonic map of the study area indicating locality and metamorphic grade (KI value) of the samples analyzed (see Table 2), as well as locality and central age from fission track data. HF — Houiller Front; SBF — Subbriançonnais Front; PBC — Penninic Basal Contact; RT — Roselend Thrust.

*Table 2* Whole rock composition, Kübler Index and *b*-cell dimension of K-White mica for samples from the Frontal Penninic Units and the Dauphinois domain. Mineral abbreviations are taken from Kretz (1983); P/M — paragonite-muscovite mixed layers; X — major components, X/O — minor components, O — traces; KI and *b*-cell dimension values from the present study. * — samples containing paragonite.

| sample number | tectonic unit | stratigraphic position | rock type | Ms | Chl | P\M | Pg | Qtz | Cal | Ab | Dol | Hem | Kfs | Kübler Index (KI) | *b* (Å) |
|---|---|---|---|---|---|---|---|---|---|---|---|---|---|---|---|
| | Houiller | | | | | | | | | | | | | | |
| Si 01* | | Carboniferous | phyllite | X | X | | X | O | | | | | | 0.191° | |
| Si 02* | | Carboniferous | phyllite | X | X | | X | O | | | | | | 0.222° | |
| Si 04* | | Carboniferous | phyllite | X | X | | X | O | | | | | | 0.207° | |
| Si 05* | | Carboniferous | phyllite | X | X | O | X | O | | | | | | 0.177° | |
| Si 06* | | Carboniferous | Qtz-phyllite | X | X | O | X | X | | | | | | 0.155° | |
| Si 07* | | Carboniferous | Qtz-phyllite | X | X | O | X | X | | | | | | 0.248° | |
| Si 08* | | Carboniferous | phyllite | X | O | | X | O | | | | | | 0.153° | |
| Si 09* | | Carboniferous | Qtz-phyllite | X | X/O | O | X | X | | | | | | 0.207° | |
| Si 10 | | Carboniferous | Qtz-phyllite | X | | | | X | | O | | | | 0.205° | 9.035 |
| Si 11 | | Carboniferous | Qtz-phyllite | X | | | | X | X | | | | | 0.241° | 9.042 |
| SC26 97 | | Lower Triassic | Cal-phyllite | X | | | | X/O | X/O | | X | | | 0.152° | 9.021 |
| SC2797a | | Lower Triassic | Cal-phyllite | X | X | | | X/O | X/O | | X | | | 0.199° | 9.026 |
| | Subbriançonnais | | | | | | | | | | | | | | |
| Si1099 | | Upper Triassic | Cal-phyllite | X | | | | X | X | | X | | | 0.261° | 9.032 |
| Si1199 | | Upper Triassic | Cal-phyllite | X | X | | | X/O | X/O | | X | | | 0.290° | 9.022 |
| Si1599 | | Upper Triassic | Cal-phyllite | X | X | | | X | X | | X | | | 0.329° | 9.012 |
| Si1699 | | Upper Triassic | Cal-phyllite | X | X | | | X | | X | X | | | 0.273° | 9.017 |
| MF2969 | | Upper Triassic | Qtz-phyllite | X | ? | | | X | O | | O | | | 0.254° | |
| MF2970 | | Upper Triassic | Qtz-phyllite | X | O | | | X | O | O | O | O | | 0.245° | |
| MF2971 | | Upper Triassic | Qtz-phyllite | X | X | | | X | O | | O | | | 0.215° | |
| MF2972 | | Middle Liassic | Cal-phyllite | X | O | | | X | O | | | | | 0.334° | |
| MF2973 | | Middle Liassic | Cal-phyllite | X | O | | | X | O | | | | | 0.266° | |
| | Cheval Noir | | | | | | | | | | | | | | |
| i71* | | Calcareous Flysch | Cal-phyllite | X | X | | X | X | X | | | | | 0.235° | |
| i72 | | Calcareous Flysch | Cal-phyllite | X | X | | | X | X | O | | | | 0.249° | 9.005 |
| Si398 | | Stratified breccia | Cal-phyllite | X | O | | | X | X | O | | | | 0.193° | 9.049 |
| Si498 | | Stratified breccia | Qtz-phyllite | X | O | | | X | O | O | | | | 0.256° | 9.037 |
| Si598 | | Stratified breccia | Qtz-phyllite | X | X | | | X | O | O | | | | 0.241° | 9.046 |
| Si698 | | Stratified breccia | Qtz-phyllite | X | X | | | X | O | | | | | 0.261° | 9.058 |
| Si798 | | Stratified breccia | Qtz-phyllite | X | | | | X | O | O | | | | 0.215° | 9.042 |
| Si898a | | Stratified breccia | Qtz-phyllite | X | X | | | X | O | O | | | | 0.301° | 9.017 |
| Si898b* | | Stratified breccia | Qtz-phyllite | X | X | | | X | | | | | O | 0.359° | 9.022 |
| Si1299* | | Wild flysch | Qtz-phyllite | X | O | | X | X | | | | | | 0.161° | |
| Si1399 | | Stratified breccia | Qtz-phyllite | X | X | | | X | | | | | | 0.334° | 9.010 |
| Si1499 | | Stratified breccia | Qtz-phyllite | X | | | | X | | | | | | 0.251° | 9.036 |
| Si1799 | | Permian | phyllite | X | O | | | X/O | | X | | | | 0.184° | 9.042 |
| Si1899 | | Permian | phyllite | X | X | | | X/O | | X | | | | 0.181° | 9.050 |
| SC4597* | | Wild flysch | phyllite | X | X | | X | X/O | | | | | | 0.229° | |
| SC499 | | Wild flysch | phyllite | X | X/O | | | X/O | | | | | | 0.219° | 9.015 |
| | Dauphinois | | | | | | | | | | | | | | |
| Si298 | | Lower Liassic | phyllite | X | X | | | X | | | | | O | 0.158° | 8.996 |
| Si198a | | Lower Liassic | Cal-phyllite | X | X | | | X | X | | | | | 0.249° | 9.017 |
| Si198b | | Lower Liassic | Cal-phyllite | X | O | | | O | X | | | | | 0.239° | 9.009 |

and Cheval Noir units) and for 3 samples from the Dauphinois domain (Figs. 3 and 4 and Table 2). Sample localities and data concerning metamorphic grade are indicated in Table 2 and Figs. 3 and 4. The *b*-cell dimension of the K-white mica was measured on 24 of the 40 samples used for KI measurements (see Table 2). 21 samples are from the FPU and 3 samples from the Dauphinois domain. The selected samples present KI values ranging from the epizone to the lower anchizone.

### *3.1. Methodological aspects*

#### *3.1.1. Sampling*

Foliation and cleavage visible in the 37 samples selected for this study in the FPU (see Fig. 3 and Table 2 for location and description of the samples, respectively) are related to the first two deformation phases D1 and D2. As will be discussed later, a possible effect of the third deformation phase D3 on the IC and the *b*-cell dimension of K-white mica cannot be excluded, especially for

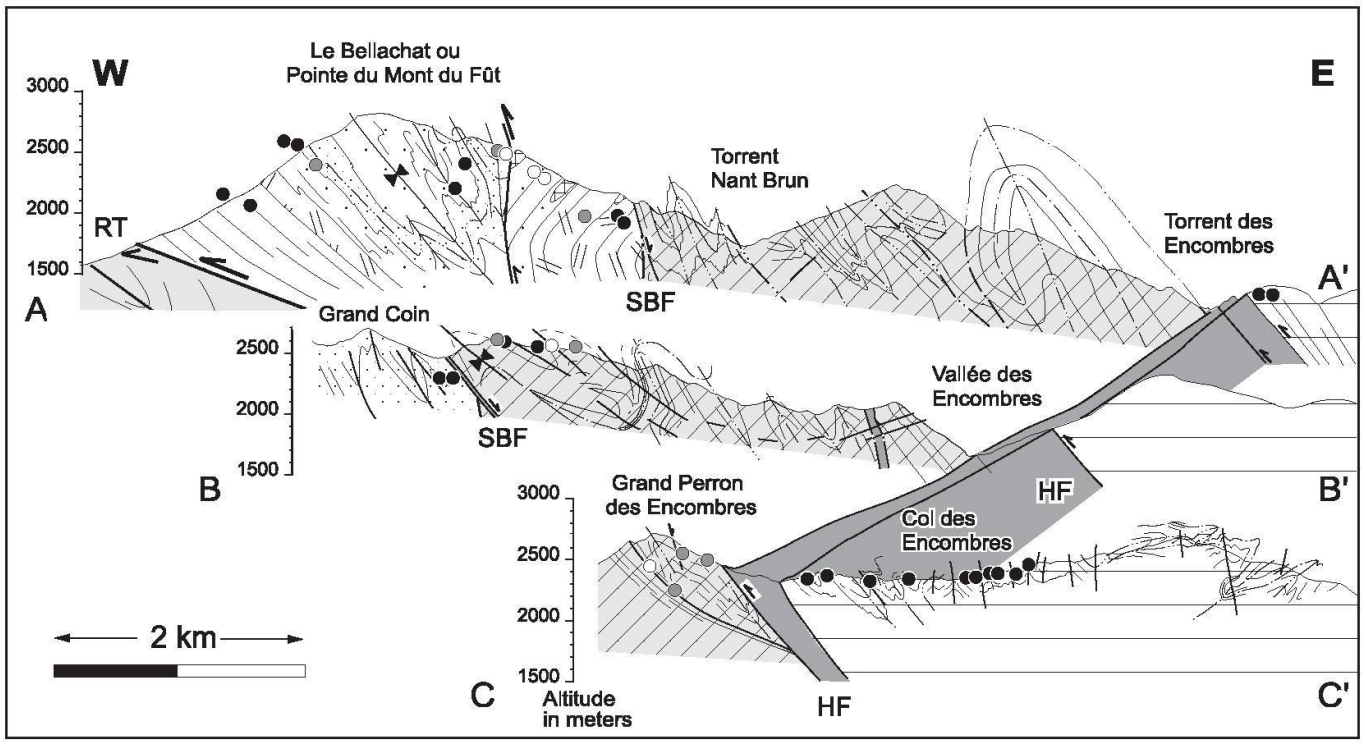


*Fig. 4* Geological cross sections (for location see Fig. 3) with KI data projected onto the cross section. The Houiller Front (HF) is shown for reference. Legend as for Figure 3.

samples from the Subbriançonnais and Cheval Noir units. The tectonic units investigated consist of different stratigraphic formations, and these do not overlap in terms of age or lithology. Therefore, it was not possible to collect and analyze samples of the same lithology over the entire studied area. Samples with detrital micas visible in hand specimen and/or weathered specimens were avoided.

Originally, the measurement of the *b*-cell dimension of K-white mica for estimating pressures was proposed for epizonal rocks with phyllitic and Qtz-phyllitic composition (Sassi and Scolari, 1974). However, Pandan et al. (1982) extended its application to high anchizonal rocks. Most samples analyzed in this study have bulk compositions that fall into the fields of phyllite or Qtz-phyllite, but calc-phyllites were also used. The *b*-values obtained from calc-phyllitic samples do not strongly differ from those of other samples from the same units (see Table 2). Samples containing significant amounts of paragonite were not used (Sassi and Scolari, 1974).

### *3.1.2. Sample preparation*

Samples were cleaned with a steel brush, crushed into small pieces with a hammer and ground in a tungsten-carbide swing-mill for up to 30 s. Carbonate was removed by treatment with 5% acetic acid and by washing with deionized water. The < 2 μm fraction was obtained using differential settling tubes and millipore filters with a pore size of 0.1 μm. The clay fraction was then Ca-saturated with 2N $CaCl_2$. Oriented slides were prepared by pipetting the suspension onto glass slides (≈ 5 mg/cm$^2$) and air-dried. For the determination of the *b*-cell dimension of K-white mica, randomly oriented samples were prepared according to the technique proposed by Dalla Torre et al. (1994).

### *3.1.3. Measurements of Illite crystallinity and K-white mica b-cell dimension*

Measurements of illite crystallinity were undertaken on a D5000 Bruker-AXS (Siemens) diffractometer. Instrumental conditions were chosen as follows: CuKα radiation, 40 V, 30 mA, automatic divergence slits (primary and secondary V20) with a secondary graphite monochromator. Illite crystallinity (IC) was measured using the software "DIFFRAC plus" (Socabim). The IC index refers to the first illite basal reflection. For samples containing paragonite (see Table 2), the IC was measured using the software "Profil Fitting". The full width at half maximum intensity (FWHM) of the first (001) and fifth (005/0010) illite reflections were measured using a Split Pearson function (background previously subtracted). When paragonite was present, a deconvolution was performed on the first peak of illite in order to separate illite and paragonite peaks.

The IC values were transformed to Kübler Index values (KI) by using a correlation with the standard samples of Warr and Rice (1994). KI was

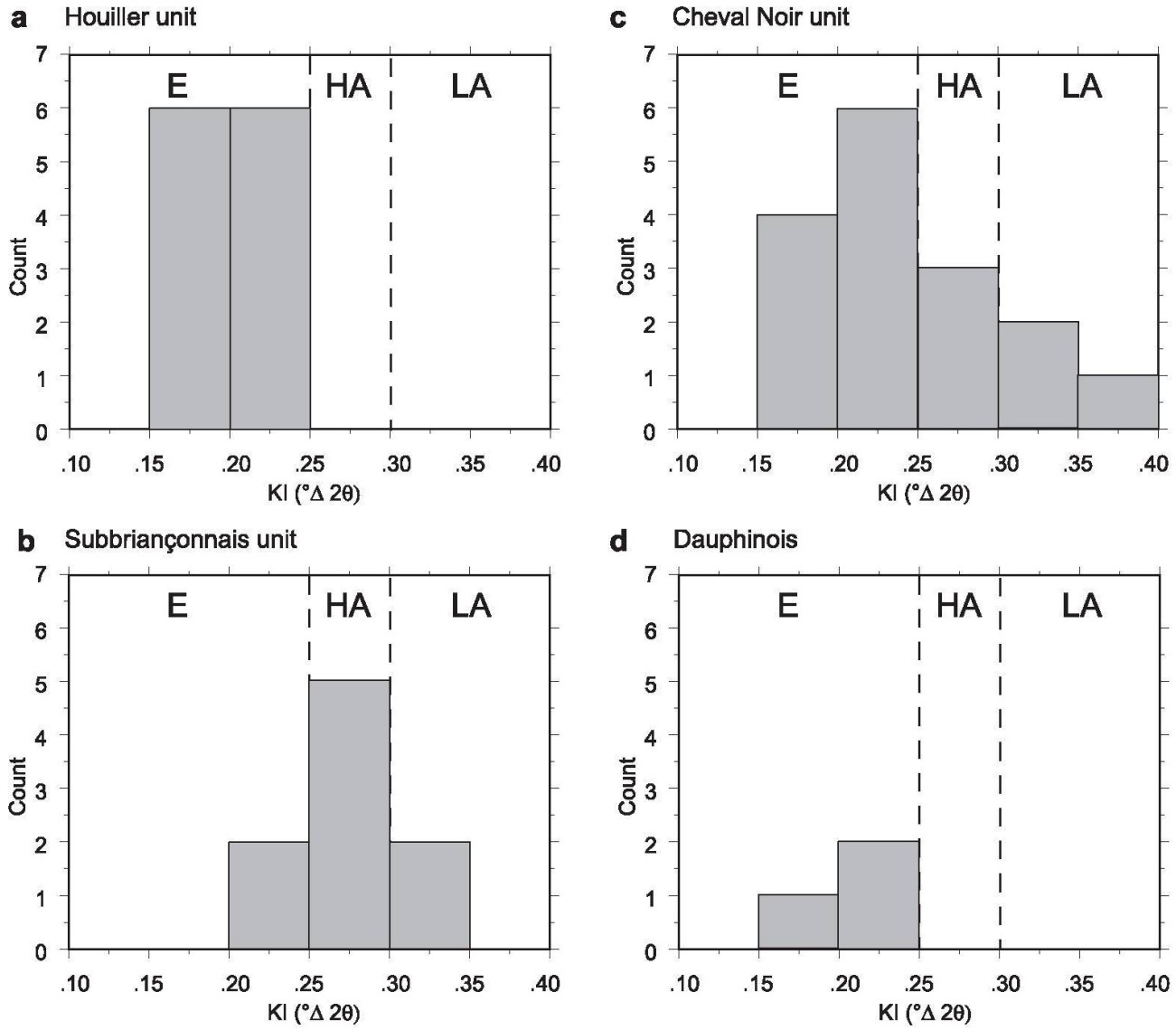


*Fig. 5* Histograms of the KI data obtained from the four different tectonic units. (a) Houiller unit; (b) Cheval Noir unit; (c) Subbriançonnais unit; (d) Dauphinois domain. E — epizone; HA — high anchizone; LA — low anchizone. The limits between E and HA (KI = 0.25 Δ°2θ), and HA and LA (KI = 0.3 Δ°2θ) are stippled and drawn after Frey and Robinson (1999).

used to define the limits of metamorphic zones, and the transition values were chosen as follows: KI = 0.25 Δ°2θ for the epizone to high anchizone boundary, KI = 0.30 Δ°2θ for the high anchizone to low anchizone boundary and KI = 0.42 Δ°2θ for the low anchizone to high diagenetic zone. For samples containing paragonite (see Table 2), the fifth reflection peak of illite (i.e. the 005/0010 illite peak at ca. 45 °2θ) was used, and the data were subsequently converted to KI by using a correlation factor for the D5000 Bruker-AXS (Siemens) diffractometer determined by David Schmid (pers. comm.). In order to estimate replication errors, 10 different air-dried slides were prepared and measured regarding samples Si10, Si1099 and Si498: the calculated error (Δ2θ) was +/– 0.015° for Si10 (Houiller unit), +/– 0.025° for Si1099 (Subbriançonnais) and +/– 0.03° for Si498 (Cheval Noir).

The K-white mica *b*-cell dimension was measured by XRD on non-oriented slides by using the d (060) peak. The position of the quartz d (211) peak was used as an internal standard.

### *3.2. Results*

#### *3.2.1. Illite crystallinity data (Kübler Index)*

From the Houiller unit the KI was determined on 12 samples (Fig. 5a). Ten of them are Carboniferous pelites (see Fig. 3 and Table 2), and 2 (i.e. SC2697 and SC2797a) come from thin pelitic strata that are interbedded with Lower Triassic dolomite (see Fig. 3 and Table 2). All of these samples yield epizonal metamorphic conditions (Fig. 5a).

In the Subbriançonnais unit the metamorphic conditions range from low anchizone to epizone

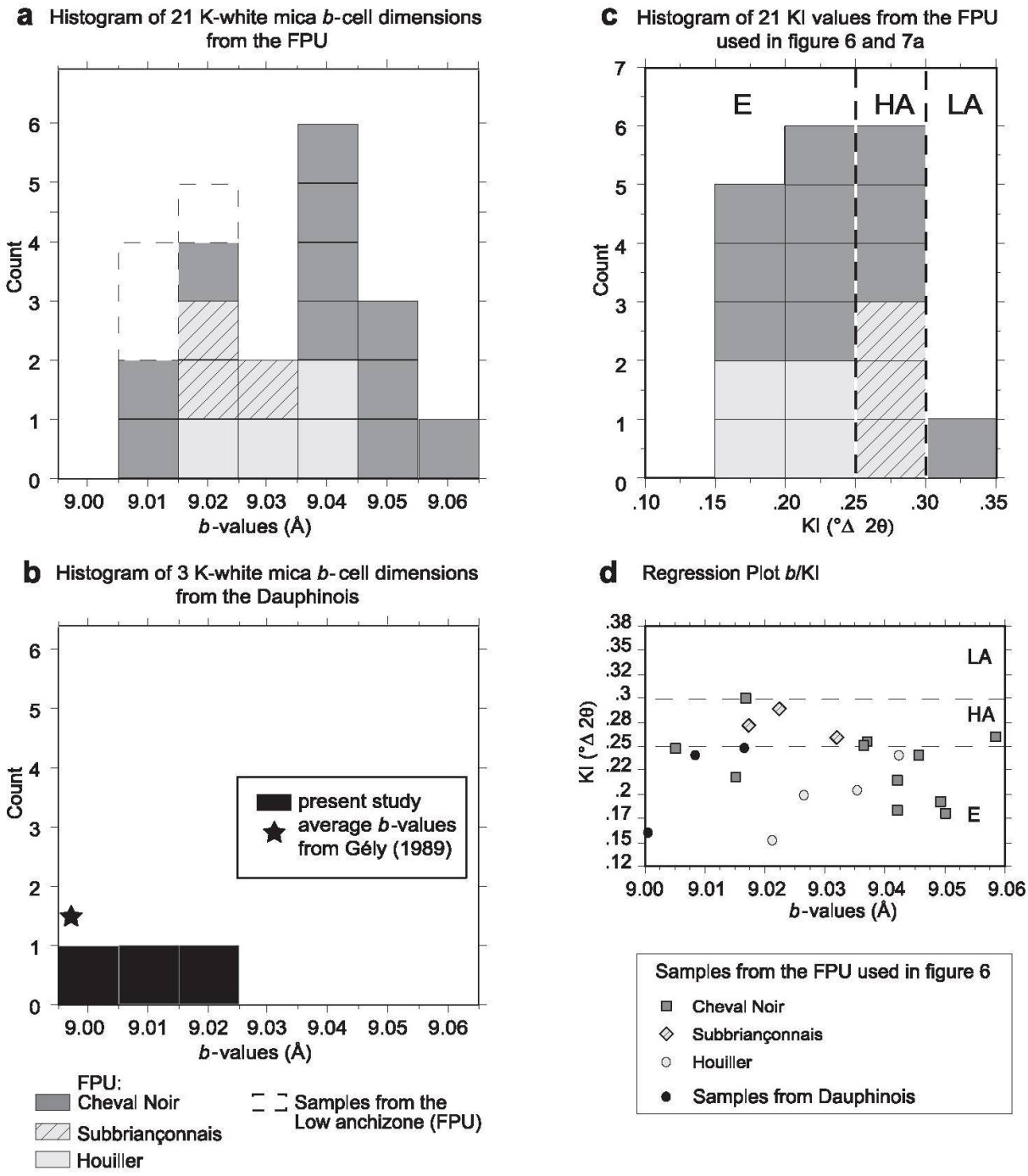


*Fig. 6* (a) Frequency histograms of the 18 $b_0$-values from the Houiller, Cheval Noir and Subbriançonnais units (same data as plotted in Fig. 7). The three $b_0$-values obtained from low anchizonal samples are shown as dashed lines. (b) Frequency histograms of the 3 K-white mica *b*-cell dimension values from the Dauphinois domain. (c) Frequency histograms of the 18 KI values from the Houiller, Cheval Noir and Subbriançonnais units, obtained on those samples analyzed for $b_0$-values and used for plotting Figs. 6a and 7. (d) KI versus *b*-cell dimension values of K-white mica for all 18 samples from the Houiller, Cheval Noir and Subbriançonnais units used for calculating the cumulative curve of Fig. 7 and for the 3 samples from the Dauphinois.

(Table 2). A peak in the distribution of KI-values is observed at high anchizonal values (Fig. 5b). Figure 5b also clearly shows that KI values for the Subbriançonnais are significantly higher (i.e. metamorphic conditions lower) when compared to those from the Houiller unit (Figs. 2 and 5a).

The 16 KI values from the Cheval Noir unit range from epizone to low anchizone (Table 2 and Fig. 5c). 14 of these samples are from Tertiary flysch and breccias, 2 samples from the Permian substratum. Data from this unit are less homogeneous than in the Houiller and Subbriançonnais units, even though that KI values of many of these samples indicate epizonal grade (see Fig. 3 and Table 2). The histogram in Fig. 5c indicates that many values lie close to the epizone-high anchizone boundary. However, despite this clear maximum in the histogram, the distribution of the

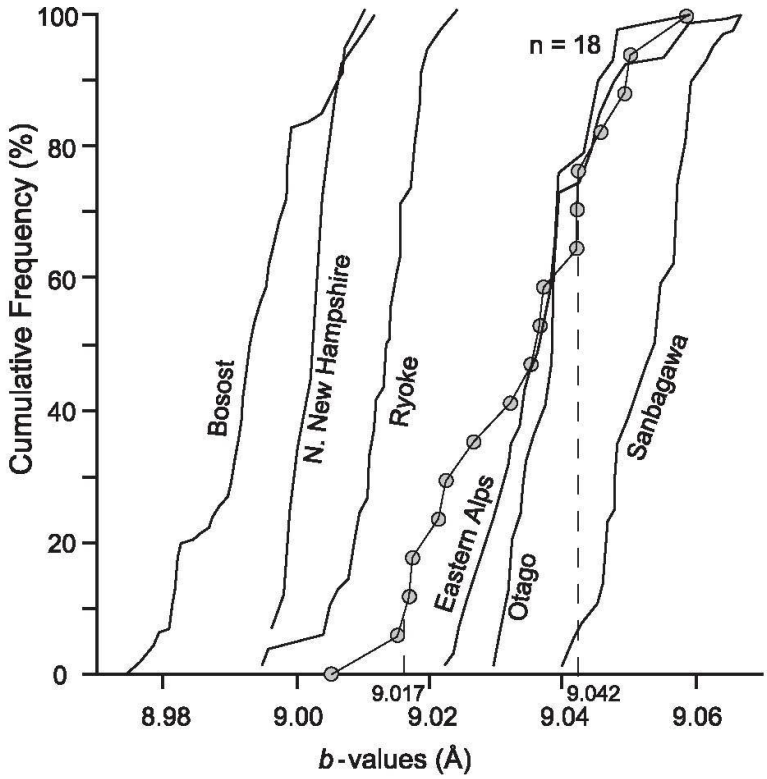


*Fig. 7* Cumulative curve of *b*-cell dimensions of K-white mica for 18 high anchizonal and epizonal samples from the Frontal Penninic units (line with circles). Reference curves (black lines) are from Sassi and Scolari (1974) and Sassi (personal communication, 1999).

KI values is very broad. As visible from Figs. 3 and 4, this broad distribution does not reflect a simple metamorphic gradient within this unit (see discussion). However, the three samples from the Cheval Noir unit which yield low anchizonal values (Si898a, Si898b and Si1399) all come from one small area (see Fig. 3). These latter values may be due to retrograde metamorphism related to D3 thrusting or to weathering not visible in the hand specimen. In fact, the area where these samples were taken (Figs. 3 and 4) is intensely tectonized due to a minor D3 thrust and lies relatively close to the major late stage normal fault, which separates the Cheval Noir from the Subbriançonnais unit. These D3 tectonic contacts may explain the high KI values observed. Overall, despite some anomalous values, a metamorphic grade near the transition from high anchizone to epizone is deduced for the Cheval Noir unit (Fig. 2). These new data indicate slightly higher conditions, compared to the anchizonal conditions proposed for this unit by earlier studies (Deharveng et al., 1987; Aprahamian, 1988).

KI was also measured on three samples collected in the Dauphinois domain near Col de la Madeleine. All three samples indicate epizonal metamorphic conditions. The KI values are compatible with the temperatures estimated by Vidal et al. (1999) for the Dauphinois domain in this area.

In summary, the results on illite crystallinity from the FPU south of Moûtiers indicate significant differences in metamorphic grade for the different tectonic units (Figs. 2 and 3).

### *3.2.2. K-white mica b-cell dimension*

The *b*-cell dimension of K-white mica was calculated for 21 samples from the FPU (Table 2), most of them ranging from the epizone to the higher anchizone. Three of them are characterized by low anchizonal conditions (i.e. Si898b, Si1399, Si1599, see Table 2) for which the method is not applicable. Hence these 3 *b*-values were not used to evaluate the FPU metamorphic conditions, although they appear compatible with the other results obtained (see Table 2 and Fig. 6a). Sample Si898a displays KI values near the high to low anchizone boundary and hence it was plotted in Figs. 6a and 7, together with the other 17 samples from the FPU.

The *b*-cell dimensions for all these 18 samples, ranging between 9.005 and 9.058 Å, were plotted in a histogram, which also contains information on the tectonic position (Fig. 6a). Two clear peaks are visible at 9.017 Å and 9.042 Å, respectively. Specimens from the Cheval Noir unit have preferentially higher *b*-values; those from the Subbriançonnais unit have lower *b*-values, while the specimens from the Houllier unit exhibit a large

spread in *b*-values. The mean K-white mica *b*-cell dimensions calculated for each of the tectonic units (not using lower anchizonal samples) are 9.031 Å for the Houiller unit, 9.024 Å for the Subbriançonnais unit, and 9.037 Å for the Cheval Noir unit. Despite these differences, the *b*-values from the individual tectonic units cannot be clearly separated into separate groups. Therefore, and in view of the common tectonic history of the three tectonic units, the 18 *b*-values have been lumped when plotting the cumulative frequency curve shown in Fig. 7.

It is customary to plot *b*-values as cumulative frequency curves (Fig. 7) in order to present and compare K-white mica *b*-cell dimension data (Sassi and Scolari, 1974). The ordinate of this plot indicates cumulative frequency, whereby the number of samples (i.e. n=18) is taken as 100%; the abscissa gives the measured length of the K-white mica *b*-cell dimension. K-white mica *b*-cell dimensions are known to increase with increasing pressure (Sassi and Scolari, 1974). Standard cumulative frequency curves obtained by Sassi and Scolari (1974) are plotted for comparison in Fig. 7. The curves for the Bosost and New Hampshire areas are typical for HT/LP metamorphism, those for the Eastern Alps and the Otago massif are characteristic for Barrovian conditions, while the Sanbagawa curve is typical for LT/HP terranes. Figure 7 suggests that the cumulative frequency curve obtained for the FPU indicates Barrovian metamorphic conditions. The slope of the curve is a measure of the homogeneity in the determined values. Since the FPU curve is flatter than that of the standard curves, it is concluded that the FPU data set is more inhomogeneous.

Returning to the histogram of Fig. 6a, with the data plotted in Fig. 7 in mind, it becomes likely that the first peak around 9.017Å is representative for Barrovian type metamorphism, while the second one at 9.042 Å does indicate higher pressure conditions (Sassi and Scolari, 1974). The KI values of the samples selected for measurement of K-white mica *b*-cell dimensions range from high anchizone to epizone, with a maximum at the boundary between epizone-high anchizone (Fig. 6c). Hence, the homogeneous distribution of the KI values is in contrast with the distribution of the K-white mica *b*-cell dimension values, characterized by two clear maxima, which do not correspond to the mean value (~9.032 Å) of the cumulative frequency curve. Interestingly, values corresponding to this mean value are practically absent.

In Fig. 6d, where the K-white mica *b*-cell dimensions are plotted against the KI values, it becomes apparent that differences of K-white mica *b*-cell dimension within the FPU do not vary as a function of the KI values. Therefore, the two maxima in the distribution of *b*-values indicated in Fig. 6a are best explained by a two-phase tectono-metamorphic history, with the first event occurring at relatively higher pressure conditions than the second event (see discussion).

In order to check this hypothesis, three K-white mica *b*-cell dimension values were also measured for the epizonal samples (Si198a/b and Si298) from the Roselette–la Madeleine unit (Dauphinois domain). It is known that this unit is only affected by one deformation phase, corresponding to the third deformation phase (D3) in the FPU, post-dating peak pressure conditions (Ceriani, 2000; Ceriani et al., 2001). The results, depicted on the histogram of Fig. 6b, do indeed indicate smaller $b_0$-values and hence lower pressures. Gély (1989) also obtained *b*-values around 9.000 Å for the Dauphinois domain in this same area. All of this suggests that D1 and D2, responsible for the main deformation in the FPU, but absent in the Dauphinois (see Table 2), was characterized by a relatively higher pressure compared to the pressures prevailing during D3.

## 4. Fission track analysis

### *4.1. Fission track data methodology and data collection*

Annealing of fission tracks occurs at 90 ± 30 °C in apatite (e.g. Green et al., 1989) and at 240 ± 60 °C in zircon (Yamada et al., 1995). The temperature intervals over which fission tracks are only partially annealed are referred to as "partial annealing zones". So far several versions of such temperature ranges defining the zircon partial annealing zone have been published (see discussions in Fügenschuh and Schmid, 2003, and Tagami et al., 1996). The estimate of Tagami et al. (1998), based on experimental studies and compilations of in situ measurements (e.g. borehole data) appears most appropriate for our study area suggesting a temperatures range between 200 °C and 320 °C for the zircon partial annealing zone. Given the metamorphic grade indicated by KI values (i.e. upper anchizone and epizone) the zircon fission tracks yield potentially important information for better defining the peak temperatures reached within the FPU of our study area.

The fission track ages from 14 samples are presented in Figs. 3 and 8. These data cover all the FPU units, from the Houiller unit to the Cheval Noir unit. They are part of a total of around 100 fission track data recently measured in the West-

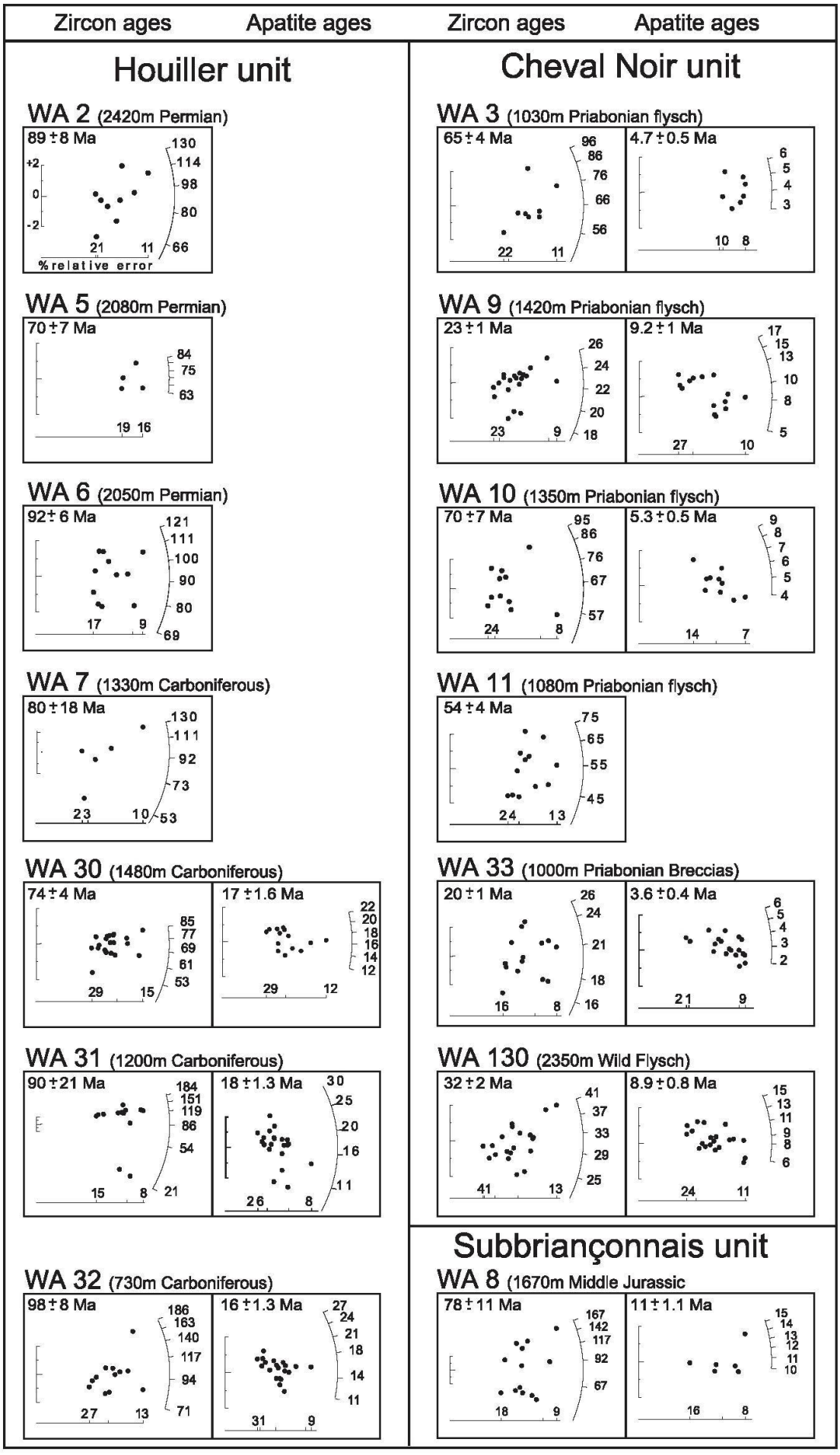


*Fig. 8* Zircon and apatite fission track central ages (± 1σ) together with radial plots (Galbraith, 1990). Sample localities are depicted in Fig. 3.

ern Alps, more specifically in the region between the Pt. St. Bernard pass (NE of Bourg St. Maurice in Fig. 1) to the north and the Arc valley to the south (Fügenschuh et al., 1999; Fügenschuh and Schmid, 2003). Fission track data are also available from the Belledonne and Chatelard massifs (see Fig. 3). The Chatelard massif is characterized by fully annealed apatites and zircons, yielding cooling ages of about 10–15 Ma (Fügenschuh and Schmid, 2003; Fig. 3) for zircon and about 5 Ma for apatite (Lelarge, 1993; Fügenschuh and Schmid, 2003; Fig. 3). From the Belledonne massif only apatite fission track data are available (Lelarge, 1993) indicating full annealing and cooling ages of about 5 Ma.

### *4.2. Results*

The 6 samples from the Cheval Noir unit were collected in Priabonian sediments (Fig. 3). The youngest zircon fission track ages were found in samples WA 33 and WA 130 taken from pebbles of pre-Triassic age in the basal breccia/olistolith horizon. Their central zircon ages are 20 and 32 Ma, respectively, i.e. younger than the age of deposition. The oldest dated grains in sample WA 130 (Valbuche area) are 40 Ma old, which corresponds to the supposed age of deposition. All single grain zircons in the other sample from the Arc valley (WA 33) are younger than Priabonian in age. The data obtained on these two samples clearly indicate that the basal part of the Cheval Noir unit was subjected to temperatures of the order of 320 °C (upper limit of the annealing zone after Yamada et al., 1995), leading to an (almost) total annealing of all zircon fission tracks. Final cooling of sample WA 33, as evidenced by the youngest zircon single grain ages (13 Ma) and by the apatite fission track central age of 3.6 Ma is very similar, and most likely linked to the cooling and exhumation of the nearby outcropping Belledonne and Chatelard external massifs.

All samples from the stratigraphically younger Priabonian flysch (WA 3, WA 10 and WA 11 in Figs. 3 and 8), except for sample WA 9, yielded apparent zircon fission track central ages older than the age of deposition. Samples WA 3, WA 10 and WA 11 display a large scatter in single grain ages from Cretaceous to Eocene/Oligocene. Therefore these samples, collected in a relatively higher stratigraphic position compared to the basal breccias, were possibly subjected to only minor partial annealing. The depth dependence of the degree of annealing can also be seen in samples WA 10 and 11, taken at 300 m differences in elevation. The topographically lower sample WA 11 not only yields a younger central age but it also contains single grains as young as Priabonian in age.

Within the Subbriançonnais unit only one sample (WA 8, see Figs. 3 and 8) could be dated. This sample, from south of the Maurienne valley, yielded a central zircon age of 78 Ma and a central apatite age of 11.4 Ma. While the apatite age represents a cooling age the zircons have obviously not been fully annealed. At least two age populations can be seen, one defined by Cretaceous ages and another, comprising six grains, with an age of 50 Ma (Fig. 8). This sample indicates that maximum temperatures in the Subbriançonnais might not have exceeded 300 °C and that final cooling started after the late Eocene. However, one sample is insufficient to draw firm conclusions.

The 7 samples from the Houiller unit were all collected in Carboniferous coarse-grained sandstones. All samples yielded apparent apatite and zircon fission track central ages (Figs. 3 and 8) younger than the age of deposition (i.e. ~300 Ma). Zircon fission track central ages range from 70 to 98 Ma, indicating an incomplete Tertiary annealing. The single grain ages scatter widely, the older grains yielding Lower Cretaceous and Jurassic ages (i.e. from ~130 to ~180 Ma, WA2, WA7 WA31 and WA32) while the youngest grains gave ages of around 20–30 Ma (WA30 and WA31). This big scatter indicates that the Houiller unit was subjected to temperatures in the range of 200 °C to 320 °C during Alpine orogeny (partial annealing zone of zircon after Tagami et al., 1998). Furthermore, the youngest Tertiary single grain ages (20–30 Ma) reflect that the Houiller unit remained within the 200 to 320 °C temperature range until Oligo–Miocene time.

The 7 samples from the Houiller unit provided only three apatite fission track ages of 16, 17 and 18 Ma (samples WA 32, WA 30 and WA 31 respectively). Apatite in these samples presents homogenous single grain age distributions (Fig. 8), indicative of fully annealed samples, hence the data are interpreted as cooling ages.

## 5. Discussion

### *5.1. Comparison of Kübler index and fission track data*

KI values within the FPU indicate differences in metamorphic conditions (primarily temperature) between the three units. However, KI only provides an approximate temperature range and cannot be used as a precise geothermometer (Frey, 1987; Essene and Peacor, 1995). In spite of this, attempts have been made to relate KI values to

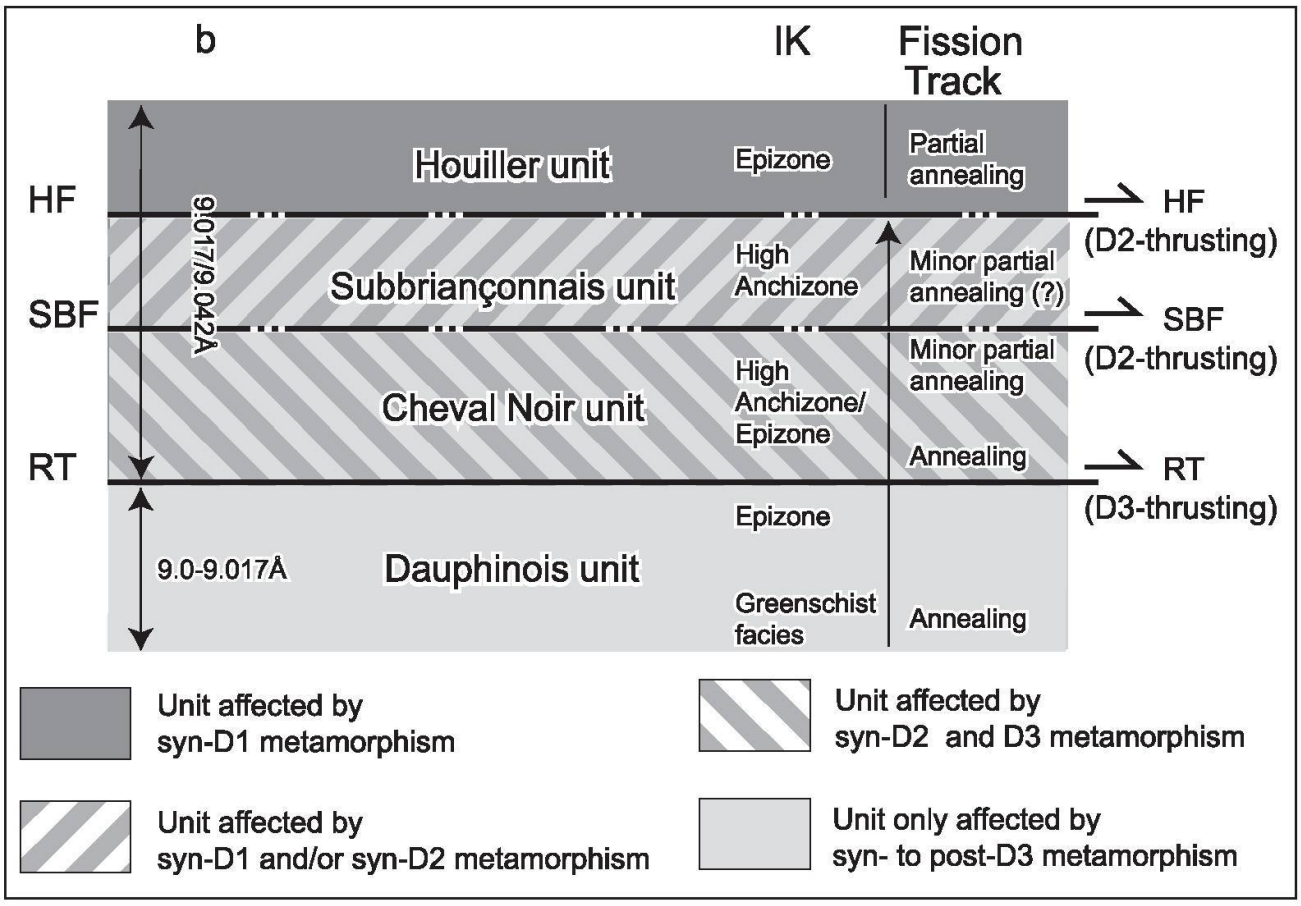


*Fig. 9* Correlation of metamorphism and deformation for the studied units. HF — Houiller Front; SBF — Subbriançonnais Front; RT — Roselend Thrust.

absolute temperatures. This was done in different low-grade metamorphic units by comparing the KI data with other geothermometers (Ferreiro Mählmann, 1996). Here we apply that calibration to the FPU and compare the results with fission track data from the same units. This allows to better define the range of temperatures to which the FPU were subjected during their tectonic evolution.

The KI values indicate that the Houiller unit underwent epizonal metamorphic conditions (Fig. 5a). According to Ferreiro Mählmann (1996) epizonal conditions correspond to temperatures higher than 270–310 °C. However, the fission track data from the same unit (see Fig. 8) show that the zircons only underwent partial annealing, i.e. that temperatures were lower than 320 °C (Tagami et al., 1998). Consequently, the comparison of KI and fission track data leads to the conclusion that the Houiller unit was subjected to temperatures higher than 270°C, but lower than 320°. Neither KI nor fission track data reveal the presence of a metamorphic gradient from E to W within the Houiller unit (Fig. 4).

For the Subbriançonnais unit only one sample was analyzed with the fission track method. Therefore a comparison with KI data is hardly possible. The KI data reflect high anchizonal condition which, according to Ferreiro Mählmann (1996), represents a temperature range of 250 to 270–310 °C. To summarize, the data presented here indicate that both units underwent peak temperatures of a similar range, i.e. 250–310 °C (Subbriançonnais) and 270–320 °C (Houiller). Comparison of KI data (Figs. 5a and b) from the two units clearly indicate that, within this temperature range, the Subbriançonnais was subjected to lower temperatures in comparison to the Houiller unit.

In the Cheval Noir unit the KI data indicate a metamorphic grade near the transition from high anchizone to epizone (Fig. 5c). Based on this, the temperatures are expected to be lower than in the Houiller unit, but higher than in the Subbriançonnais units, comprising a range of 270–310 °C (Ferreiro Mählmann, 1996). Fission track data (Fig. 8), as discussed in the previous chapter, show the presence of a metamorphic gradient within the Cheval Noir unit. Completely reset zircon fission track ages are observed in the samples from the stratigraphic base of the unit (Figs. 3 and 8, samples WA 33 and WA 130) where the KI data indicate epizonal conditions (Fig. 3 and Table 2). Instead, fission track data from the stratigraphic top

of the unit (i.e. samples WA3, WA 10 and WA 11 from the Priabonian calcareous flysch, Figs. 3 and 8) show minor partial annealing only. From these fission track data, temperatures around 320 °C are inferred for the base, while temperatures around 200 °C or slightly higher are inferred for the top of the Cheval Noir unit. From the KI data alone this metamorphic gradient is not as clearly visible (Fig. 3), but the KI values are compatible with the fission track data. In fact, with the exception of samples Si398 and Si798, all samples with the higher KI values are from the stratigraphic base of the Cheval Noir unit (i.e. the pre-Tertiary substratum and the wild-flysch). These samples (i.e. SC4597, SC499, Si1299, Si1799, and Si1899) yield a mean KI value of 0.195, compatible with the temperature around 320 °C estimated by using fission track for this part of the unit.

We conclude that zircon fission track and KI data show compatible results over the entire study area. Both methods indicate the same trend in temperature conditions between the different FPU, and both methods show that the Houiller unit was subjected to higher temperatures than the other FPU. Concerning the Houiller unit, the comparison of KI and fission track data allows a better definition of the temperatures to which this unit was subjected.

### *5.2. Tectono-metamorphic evolution of the FPU*

We now integrate the available metamorphic data from the FPU with the deformation history deduced from field mapping (Ceriani, 2001; Ceriani et al., 2001). This allows us to deduce some important conclusions concerning the tectono-metamorphic evolution of the FPU.

A first important result provided by KI and fission track data is the fact that the Houiller unit, as a relatively higher tectonic unit, exhibits higher (epizone) metamorphic conditions (see Figs. 2, 3 and 5a) when compared to the underlying Subbriançonnais (high anchizone, Figs. 2, 4 and 5b) and Cheval Noir (high anchizone/epizone, Figs. 2, 4 and 5c) units. The Houiller Front (see Figs. 2, 3 and 4), a thrust that carried the Houiller unit on top of the Subbriançonnais unit, was active as a NNW-directed transpressive thrust during the second tectonic phase D2 (Figs. 4 and 9 and Table 1). This suggests that epizonal metamorphic conditions in the Houiller unit were already established during D1, before the Houiller was finally emplaced on top of the Subbriançonnais unit. Hence, the epizonal metamorphic conditions in the Houiller unit are regarded as being transported along the D2 Houiller Front.

In view of the sparse data from the Subbriançonnais unit no inferences can be made, from the KI data alone, regarding the tectono-metamorphic significance of the Subbriançonnais Front that separates the Subbriançonnais unit from the Cheval Noir unit. Field evidence in the Valbuche area (Fig. 2) instead indicates that top-to-the-north thrusting along the Subbriançonnais Front can be correlated to the second regional deformation phase D2 affecting the FPU (Ceriani et al., 2001). In the Cheval Noir unit, characterized by two deformation phases only (Table 1), D2 corresponds to the first penetrative schistosity, marked by very fine-grained white mica, chlorite, quartz and albite, and related isoclinal folds developed in the entire unit. Overthrusting of the Subbriançonnais unit along the Subbriançonnais Front (Fig. 10b) during D2 produced a synform in the Cheval Noir unit, with the Priabonian Flysch in the core. The reverse limb of this major synform is only preserved north of the Valbuche area (Figs. 3 and 4) where F3 folds refold an already reversed stratigraphic series. During the third regional deformation phase D3, the Cheval Noir unit was overthrusted on top of the Dauphinois domain along the WNW-directed Roselend thrust. A major F3 synform developed in the Cheval Noir unit during D3 (Figs. 4 and 10a).

As discussed in the previous section, zircon fission track ages clearly show a metamorphic gradient in the Cheval Noir unit, with the younger sediments showing a lower metamorphic grade than the older one. The present day positions of samples WA33, WA3 and WA130 indicate that the large F3 synform post-dates the metamorphic peak (see Fig. 10a). In fact, sample WA3 from the core of this synform yields a central age older than the stratigraphic age, while the samples in the limbs (WA33 and WA130, Fig. 10a) present central ages younger than the stratigraphic age. Figure 8 also shows that the samples from the limb of this synform, associated with a higher degree of metamorphism, display an age versus altitude correlation. This indicates that most of the exhumation post-dates the formation of this F3 fold. From the zircon fission track cooling ages a pre-Late Oligocene peak of metamorphism can be inferred. Thus the metamorphic peak formed during the regional D2, in Priabonian time.

Based on the KI and fission track data alone, it is not always possible to distinguish the metamorphic effects of the first and second phases (D1 and D2) from those of the third (D3) deformational phase in the FPU. Further information for correlating metamorphism with deformation is provided by the K-white mica *b*-cell dimensions that are a function of pressure conditions prevailing dur-

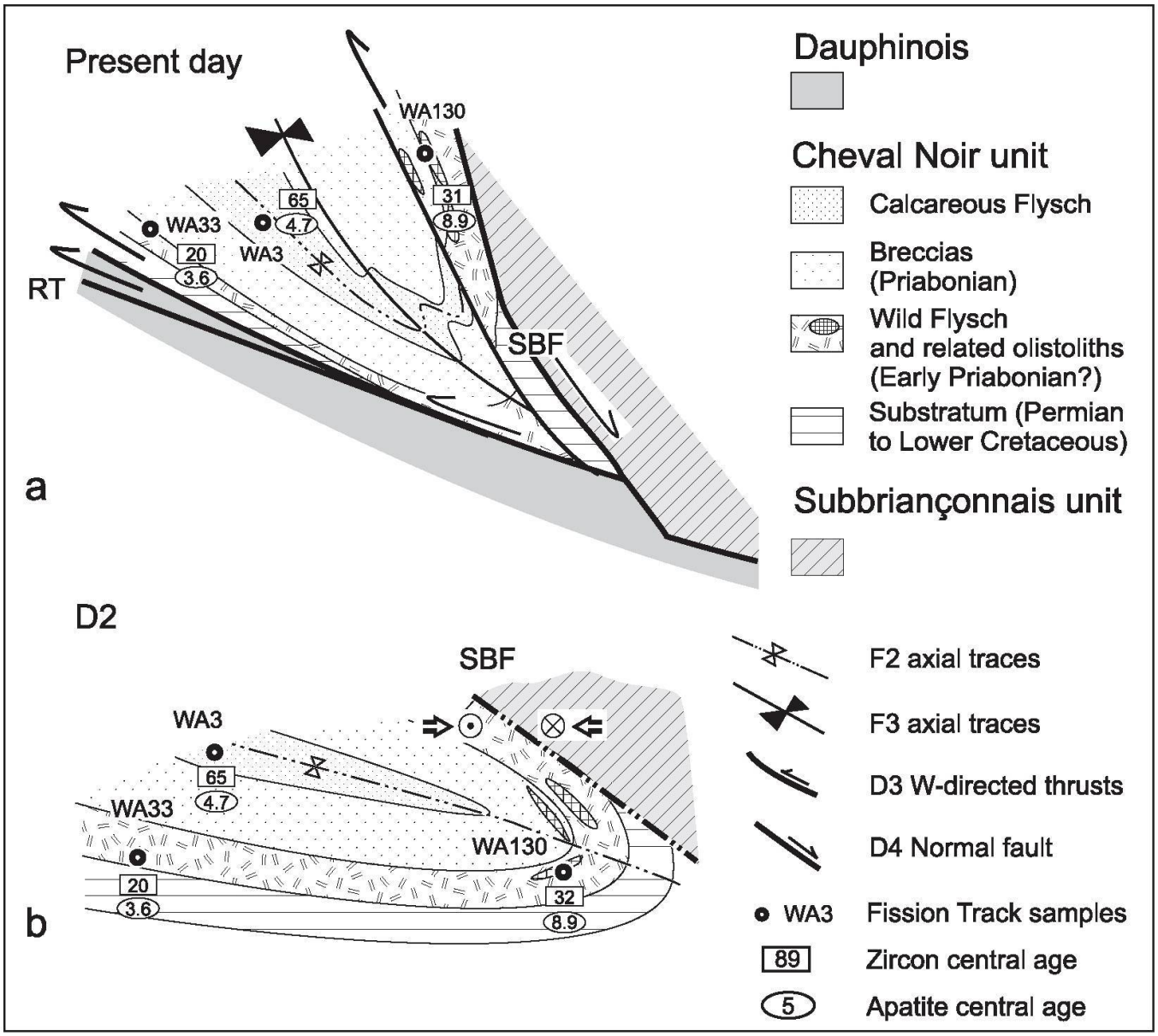


*Fig. 10* (a) Schematic profile showing the present day position of samples WA3, WA33 and WA130. (b) Sketch of the Cheval Noir unit during the last stages of D2, indicating the inferred position of samples WA3, WA33 and WA130. SBF — Subbriançonnais Front, RT — Roselend Thrust. Note that regional "D2" represents the first deformation phase in the Cheval Noir unit (see Table 1).

ing metamorphism. As pointed out earlier, the *b*-cell dimension of the K-white mica from the Cheval Noir, Subbriançonnais and Houiller units present a bimodal distribution, with peaks at 9.017 Å and 9.042 Å (Figs. 6 and 7). In contrast, the *b*-cell dimension of the K-white mica from the Dauphinois domain are uniform and in the range from 8.996 to 9.017 Å (Fig. 6b and Gély, 1989).

These data indicate that metamorphism in the FPU at least partly developed during a lower geothermal gradient (i.e. at relatively higher pressure), in contrast to metamorphism in the Dauphinois domain, where the peak around 9.042 Å is not observed. This is best explained by the superposition of the effects of a post-collisional temperature-dominated metamorphic event, which prevailed during D3 (characterized by a lower pressure), onto the effects of a pre- to syn-collisional pressure-dominated metamorphic event (correlated with D1 and D2 in Fig. 9). The metamorphic effects during D3 are mainly visible in the Dauphinois domain, characterized by clearly lower K-white mica *b*-cell dimensions compared to the FPU.

Concerning the ages of the deformation phases affecting the FPU and the Dauphinois (Table 1), the syn-D1 metamorphic peak in the Houiller unit is pre-35 Ma (Fügenschuh and Schmid, 2003) and likely to be of pre-Priabonian age (Ceriani et al., 2001). Sedimentological evidence (Ceriani et al., 2001) and fission track data (see above) indicate that the tectonic activity along the Subbriançonnais Front, and more in general the second deformation phase (D2), can be dated at Priabon-

ian (i.e. ~34–37 Ma, Table 1). The younger strata of the Priabonian flysch of the Cheval Noir unit embed large olistoliths of Subbriançonnais origin. Their emplacement is interpreted to be related to the early-D2 tectonic activity along the Subbriançonnais Front (Ceriani et al., 2001).

At the end of the Priabonian, i.e. at the end of the first stage (D1 and D2 in Table 1), the Cheval Noir, Subbriançonnais, and Houiller units were internally structured, and hence they already looked as we see them today and had already reached the metamorphic peak. In particular, the Houiller unit already occupied a position on top of the rest of the FPU. This is consistent with the apatite fission track ages that indicate earlier exhumation for this structurally highest unit (i.e. around 16–18 Ma) with respect to the Cheval Noir unit (3–11 Ma) and to the Dauphinois domain (3–6.7 Ma).

During a second stage (i.e. D3 in Table 1) of Oligocene to Early Miocene age (see Table 1) the previously stacked and structured FPU (including the Valaisan units), were overthrusted onto the Dauphinois domain along the Roselend thrust (RT) (Figs. 2, 4, 9 and Table 1). The Dauphinois domain displays a normal metamorphic gradient, with temperatures decreasing from west to east, i.e. from the base to the top of this unit (Fig. 2), metamorphic conditions decreasing from greenschist facies to epizonal conditions. This metamorphic gradient and the related low K-white mica *b*-cell dimensions are interpreted as being related to burial heating, generated by the overthrusted Penninic units along the Roselend Thrust during D3. With the aid of fission track data from the northern rim of the Pelvoux massif (Seward et al., 1999) this thermal overprinting was dated at 24–27.5 Ma (see discussion in Ceriani et al., 2001). We conclude that the RT was active a few Ma before the age of this thermal peak.

Presently a normal metamorphic gradient is observed in the entire nappe stack between the Dauphinois domain at the base and the Subbriançonnais unit at the top (Figs. 2 and 9). This gradient covers the entire range from greenschist facies at the base to high anchizone at the top. Metamorphism in the Dauphinois domain most probably is the result of burial heating after the emplacement of the FPU along the syn-D3 RT. However, the gradient ranging from epizone to high anchizone observed in the overlying units (Cheval Noir and Subbriançonnais) had already been generated during the late stages of D2. This is supported by the higher *b*-cell dimension values of K-white mica compared to those in the Dauphinois domain. Metamorphism in the SBU probably is related to the emplacement of the Houllier unit along the Houiller Front during D2). Metamorphism in the Cheval Noir unit, on the other hand, is likely to be related to the emplacement of the SBU on top of this most external Penninic unit along the SBF during D2. The Houiller unit, lying on top of this nappe stack, does not fit into this normal metamorphic gradient. Instead it exhibits epizonal values which were transported during D2 and, hence, pre-date D2. In summary, the metamorphic overprint was heterochroneous and became younger from E to W (Fig. 9).

The tectonic and metamorphic history, as discussed so far, is further affected by post-D3 deformations. Apatite fission track data, together with fieldwork, provide evidence for this most recent evolution of the studied area. Final cooling of the Cheval Noir unit, as shown by the youngest zircon single grain ages (13 Ma in sample WA 33) and apatite fission track ages ranging from 3.6 to 9 Ma) is very similar and most possibly linked to the Miocene cooling and exhumation of the Belledonne and Chatelard external massifs (Fig. 3), related to the combined effects of Middle to Late Miocene thrusting of the external massifs onto their foreland and erosion (see discussion in Fügenschuh and Schmid, 2003). In contrast to this, sample WA 8 from the SBU (i.e. 11 Ma), as well as all the samples from the Houiller unit (WA 31: 18 Ma, WA 32: 16 Ma), record older apatite fission track ages, indicating earlier cooling and inferred exhumation of these units. Post-5 Ma normal faulting (Fügenschuh et al., 1999) represents the latest deformation event (third stage or D4 tectonic phase in Table 1) and is also observed in our study area, where it reactivates the syn-D2 SBF. This late stage normal fault may also be responsible for the slight difference in metamorphism recorded in the Cheval Noir and Subbriançonnais units, as evidenced by the KI values.

## 6. Conclusions

The tectono-metamorphic history of the FPU can be divided into three major stages (Ceriani et al., 2001): the first one is pre- to syn-collisional (D1 and D2), and the second (D3) and third (D4) one post-collisional. The metamorphism affecting the FPU south of Moûtiers is mainly related to the first stage (i.e. D1 and D2 deformation phases), although some minor effects of the post-collisional D3 phase are visible in the Cheval Noir unit and cannot be excluded for the Subbriançonnais unit.

Within the FPU south of Moûtiers the highest temperatures (~300 °C) were registered in the highest tectonic unit investigated (Houiller unit)

on one hand, and at the base of the lowest unit (Cheval Noir unit) on the other hand.

Peak metamorphic conditions in the Houiller Unit were reached before this unit was thrusted on top of the other FPU during D2. From the Priabonian onwards this unit was mainly characterized by overall slow cooling.

Metamorphism in the Cheval Noir unit is younger than in the Houiller unit. Fission track data display a vertical gradient within the Cheval Noir unit. Since this gradient was refolded during D3, we interpret the metamorphic peak in the Cheval Noir unit to be syn-D2 and related to the overthrusting of the Subbriançonnais and Houiller units. The bimodal distribution of the K-white mica *b*-cell dimension in this unit, however, suggests an influence also of D3 on the metamorphism recorded in this unit. During D3 the Cheval Noir unit (i.e. the lower of the FPU) was probably affected by temperatures in the same range as those reached during D2, but characterized by lower pressures. Concerning the Subbriançonnais unit no clear conclusions can be drawn.

The *b*-cell dimensions of K-white mica recorded in the FPU display a bimodal distribution, indicating a polymetamorphic history as a consequence of the superposition of the effects of the three deformation phases observed. The *b*-cell dimension values of K-white mica do not show major differences within the FPU units. However, the K-white mica *b*-cell dimension values from the FPU are clearly higher than the ones recorded in the Dauphinois domain, indicating that metamorphism in this most external domain occurred at low-pressure conditions only. This is corroborated by the structural observation that the Dauphinois is affected by one major phase of deformation only (i.e. D3). The metamorphic peak in the Dauphinois post-dates that of the FPU and is related to the overthrusting of the FPU along the syn-D3 Roselend thrust. The new data concerning the metamorphic evolution presented here can be nicely integrated into the tectonic reconstruction proposed by Ceriani et al. (2001). The first two phases (D1 and D2) developed during subduction of the Valaisan units and within an accretionary wedge. Metamorphism within the FPU is mainly related to these first two phases (D1 and D2). The third deformational phase (D3), developed in a post-collisional scenario, is characterized by higher geothermal gradient, i.e. by relatively lower pressures, and led to metamorphism in the footwall of the FPU, within the Dauphinois domain.

**Acknowledgements**

We thank the other members of the Basel "Western Alps team": Romain Bousquet, Stefan Bucher, Andrea Loprieno and Ghislain Trullenque for their significant contribution to this work. We also acknowledge the contribution of the late Professor Martin Frey, who introduced us into the "world" of low-grade metamorphism, and who supported us in collecting, analyzing and evaluating the data on which this paper is based. Reviews by Diane Seward and Martin Engi are gratefully acknowledged. We finally acknowledge continuous funding since 1994 of this and other studies in the French-Italian Alps by the Swiss National Science Foundation (projects 20-42132.94, 20-49558.96, 20-55559.98 and 20-63391.00).

**References**

Aprahamian, J. (1988): Cartographie du métamorphisme faible à trés faible dans les Alpes françaises externes par l'utilisation de la cristallinité de l'illite. *Geodin. Acta* **2**, 25–32.

Cannic, S., Lardeaux, J.M., Mugnier, J.L. and Hernandez, J. (1996): Tectono-metamorphic evolution of the Roignais-Versoyen Unit (Valaisan domain, France). *Eclogae geol. Helv.* **89**, 321–343.

Ceriani, S. (2001): A combined study of structure and metamorphism in the frontal Penninic units between the Arc and the Isère valleys (Western Alps): Implications for the geodynamics evolution of the Western Alps. Unpublished PhD thesis, Univ. Basel, 196 pp.

Ceriani, S., Fügenschuh, B. and Schmid, S.M. (2001): Multi-stage thrusting at the "Penninic Front" in the Western Alps between Mont Blanc and Pelvoux massifs. *Int. J. Earth Sci.* **90**, 685–702.

Debelmas, J. (1989): Carte Géologique de la France à 1/50000, Feuille 775 Modane. B.R.G.M.

Deharveng, L., Perriaux, J. and Ravenne, C. (1987): Sedimentologie du flysch des Aiguilles d'Arves (Alpes Francaises). *Géologie Alpine Mem. hors série* **13**, 329–341.

Essene, E.J. and Peacor, D.R. (1995): Clay mineral thermometry – a critical perspective. *Clays Clay Mineral.* **43**, 540–553.

Ferreiro Mählmann, R. (1996): Das Diagenese-Metamorphose-Muster von Vitrinitreflexion und Illit-„Kristallinität" in Mittelbünden und im Oberhalbstein. Teil 2: Korrelation kohlenpetrographischer und mineralogischer Parameter. *Schweiz. Mineral. Petrogr. Mitt.* **76**, 23–46.

Frey, M. (ed.)(1987): Low Temperature Metamorphism. Blackie & Son, Glasgow and London, 351 pp.

Frey, M., Desmons, J. and Neubauer, F. (eds.)(1999): Metamorphic Maps of the Alps. An Enclosure to *Schweiz. Mineral. Petrogr. Mitt.* **79/1**.

Frey, M. and Robinson, D. (eds.)(1999): Low-Grade Metamorphism. Blackwell Science, Oxford, 313 pp.

Fügenschuh, B., Loprieno, A., Ceriani, S. and Schmid, S.M. (1999): Structural analysis of the Subbriançonnais and Valais units in the area of Moûtiers (Savoy, Western Alps): paleogeographic and tectonic consequences. *Int. J. Earth Sci.* **88**, 201–218.

Fügenschuh, B. and Schmid, S.M. (2003): Late stages of deformation and exhumation of an orogen constrained by fission-track data: a case study in the Western Alps. *Geol. Soc. Am. Bull.* ***15***, 1425–1440.

Galbraith, R.F. (1990): The radial plot: graphical assessment of spread in ages. *Nuclear Tracks and Radiation Measurements* **17**, 207–214.

Gély, J.-P. (1989): Stratigraphie, tectonique et métamorphisme comparés de part et d'autre du Front Pennique en Tarentaise. Unpublished PhD thesis, Univ. Savoie, 343 pp.

Gély, J.-P. and Bassias, Y. (1990): Le Front Pennique: Implications structurales d'un métamorphisme transporté (Savoie, France). *C.R. Acad. Sci. Paris Sér. II* **310**, 37–43.

Goffé, B. and Bousquet, R. (1997): Ferrocarpholite, chloritoid and lawsonite in metapelites of the Versoyen an Petit St. Bernard units (Valais zone, Western Alps). *Schweiz. Mineral. Petrogr. Mitt.* **77**, 137–147.

Green, P.F., Duddy, I.R., Laslett, G.M., Hegarty, K.A., Gleadow, A.J.W. and Lovering, J.F. (1989): Thermal annealing of fission tracks in apatite, quantitative modelling techniques and extension to geological timescales. *Chem. Geol.* **79**, 155–182.

Jullien, M. and Goffé, B. (1993): Occurrences de cookéite et de pyrophyllite dans le schistes du Dauphinois (Isère, France): Conséquences sur la répartition du métamorphisme dans les zones externes alpines. *Schweiz. Mineral. Petrogr. Mitt.* **73**, 357–363.

Kretz, R. (1983): Symbols for rock-forming minerals. *Am. Mineral.* **68**, 277–279.

Lelarge, L. (1993): Thermochronologie par la méthode des traces de fission d'une marge passive (Dôme de Ponta Grossa, SE Brésil) et au sein d'une chaîne de collision (zone externe de l'Arc alpine, France). Unpublished PhD thesis, Univ. Joseph Fourier, 252 pp.

Loprieno, A. (2001): A combined structural and sedimentological approach to decipher the evolution of the Valais domain in Savoy (Western Alps). Unpublished PhD thesis, Univ. Basel, 285 pp.

Mullis, J., Rahn, M.K., Schwer, P., de Capitani, C., Stern, W.B. and Frey, M. (2002): Correlation of fluid inclusion temperatures with illite "crystallinity" data and clay mineral chemistry in sedimentary rocks from the external part of the Central Alps. *Schweiz. Mineral. Petrogr. Mitt.* **82**, 325–340.

Pandan, A., Kisch, H.J. and Shagam, R. (1982): Use of the lattice parameter "b0" of dioctahedral illite/muscovite for the characterization of P/T gradients of incipient metamorphism. *Contrib. Mineral. Petrol.* **79**, 85–95.

Sassi, F.P. (1972): The petrological and geological significance of the b0 values of potassic white micas in low-grade metamorphic rocks. An application to the Eastern Alps. *Tschermacks Mineral. Petrogr. Mitt.* **18**, 105–113.

Sassi, F.P. and Scolari, A. (1974): The b0 value of the potassic white micas as a barometric indicator in low-grade metamorphism of pelitic schists. *Contrib. Mineral. Petrol.* **45**, 143–152.

Schürch, M.L. (1987): Les ophiolites de la zone du Versoyen: témoin d'un bassin à évolution métamorphique complexe. Unpublished PhD thesis, Univ. Genève, 157 pp.

Serre, A., Toury, A., Rampnoux, J.-P., Martinez-Reyes, J. and Tardy, M. (1985): Individualisation de deux unités à flysch nummulitique d'origines paléogéographiques différentes au sein de „l'Ecaille ultradauphinoise des Aiguilles d'Arves" (région de Saint-Jean de Maurienne, Savoie). *C.R. Acad. Sci. Paris Sér. II* **301**, 637–642.

Seward, D., Ford, M., Bürgisser, J., Lickorish, H., Williams, E.A. and Meckel III, W.L.D. (1999): Preliminary results of fission-track analyses in the Southern Pelvoux area, SE France. *Mem. Sci. Geol.* **51**, 25–31.

Sue, C. and Tricart, P. (1999): Late Alpine brittle extension above the Frontal Pennine Thrust near Briançon, Western Alps. *Eclogae geol. Helv.* **92**, 171–181.

Tagami, T., Galbraith, R., Yamada, R. and Laslett, G.M. (1998): Revised annealing kinetics of fission-tracks in zircon and geological implications. In: Van den Haute, P. and De Corte, F. (eds.): Advances in fission-track geochronology. Kluwer Academic Publishers, Dordrecht, 99–114.

Vidal, O., Goffé, B. and Parra, T. (1999): Calibration and testing of an empirical chloritoid-chlorite exchange thermometer and thermodynamic data for daphnite. *J. Metamorphic Geol.* **17**, 25–39.

Yamada, R.T., Tagami, S., Nishimura and Ito, H. (1995): Annealing kinetics of fission track in zircon: an experimental study. *Chem. Geol.* (Isotope Geoscience Section) **122**, 249–258.

Received 27 August 2002
Accepted in revised form 8 August 2003
Editorial handling: M. Engi